Quark loop calculation of the $\gamma \to 3\pi$ form factor

Bojan Bistrović and Dubravko Klabučar
Department of Physics, Faculty of Science, Zagreb University, Bijenička c. 32, 10001 Zagreb, Croatia
(Received 29 July 1999; published 6 January 2000)

The presently experimentally interesting form factor for the anomalous process $\gamma \to \pi^+\pi^0\pi^-$ is calculated as the quark ''box'' amplitude where the intermediate fermion loop is the one of constituent quarks with the pseudoscalar coupling to pions. This also corresponds to the form factor, in the lowest order in pion interactions, of the σ model and of the chiral quark model. We give the analytic expression for the form factor in terms of an expansion in the pion momenta up to the order $\mathcal{O}(p^8)$ relative to the soft point result, and also perform its exact numerical evaluation. We compare our predictions with those of vector meson dominance and chiral perturbation theory, as well as with the scarce data available so far.

PACS number(s): 13.40.Gp, 12.38.Lg, 14.40.Aq, 24.85.+p

The analysis of the Abelian axial anomaly [1,2] shows that the $\pi^0 \to \gamma\gamma$ amplitude is exactly $T_\pi^{2\gamma}(m_\pi=0) = e^2 N_c/(12\pi^2 f_\pi)$ in the chiral and soft limit of pions of vanishing mass m_π. (Here, e is the proton charge, and $N_c = 3$ is the number of quark colors.) This amplitude $T_\pi^{2\gamma}(m_\pi = 0)$ is successfully reproduced also by the simple ''free'' quark loop (QL) calculation of the pseudoscalar-vector-vector (PVV) ''triangle,'' provided one uses the quark-level Goldberger-Treiman (GT) relation $g/M = 1/f_\pi$ to express the effective constituent quark mass M and quark-pion coupling strength g in terms of the pion decay constant $f_\pi = 92.4$ MeV. This calculation (essentially in the manner of Steinberger [3]) is the same as the lowest (one-loop) order calculation [2] in the σ model which was constructed to realize current algebra explicitly. By ''free'' quarks we mean that there are no interactions between the effective constituent quarks in the loop, while they *do* couple to external fields, presently the photons A_μ and the pion π_a. Our effective QL model Lagrangian is thus

$$\mathcal{L}_{eff} = \bar{\Psi}(i\partial\!\!\!/ - e\mathcal{Q}A\!\!\!/ - M)\Psi - ig\bar{\Psi}\gamma_5\pi_a\tau_a\Psi + \cdots, \quad (1)$$

where $\mathcal{Q} \equiv \mathrm{diag}(Q_u, Q_d) = \mathrm{diag}(\frac{2}{3}, -\frac{1}{3})$ is the quark charge matrix, and τ_a are the Pauli $SU(2)$-isospin matrices acting on the quark isodoublets $\Psi = (u,d)^T$. The ellipsis in $\mathcal{L}_{eff}$ serve to remind us that Eq. (1) also represents the lowest order terms from the σ-model Lagrangian which are pertinent for calculating photon-pion processes. The same holds for all chiral quark models (χQM)—considered in, e.g., Ref. [4]—which contain quark-meson coupling $M\bar{\Psi}(UP_L + U^\dagger P_R)\Psi$ with $P_{L,R} = (1 \pm \gamma_5)/2$. Namely, expanding $U^{(\dagger)} = \exp[(-)i\pi_a\tau_a/f_\pi]$ to the lowest order in π_a and invoking the GT relation again returns the QL model Lagrangian (1).

This simple QL model (and hence also the lowest order χQM and the σ model) provides an analytic expression (e.g., see Ref. [5]) for the amplitude $T_\pi^{2\gamma}(m_\pi)$ also for $m_\pi > 0$ (but restricted to $m_\pi < 2M$, which anyway must hold for the light, pseudo Goldstone pion), namely,

$$T_\pi^{2\gamma}(m_\pi) = \frac{e^2 N_c}{12\pi^2 f_\pi}\left[\frac{\arcsin(m_\pi/2M)}{(m_\pi/2M)}\right]^2 = \frac{e^2 N_c}{12\pi^2 f_\pi}\left[1 + \frac{m_\pi^2}{12M^2} + \cdots\right]. \quad (2)$$

Adler *et al.*, Terentev, and Aviv and Zee [6] proved that the amplitude for the anomalous processes of the type $\gamma \to 3\pi$ is related to $T_\pi^{2\gamma}(0)$ and is given by

$$F_\gamma^{3\pi}(0,0,0) = \frac{1}{ef_\pi^2} T_\pi^{2\gamma}(0) = \frac{eN_c}{12\pi^2 f_\pi^3}. \quad (3)$$

The arguments of the anomalous amplitude (3), namely, the momenta $\{p_1, p_2, p_3\}$ of the three pions $\{\pi^+, \pi^0, \pi^-\}$, are all set to zero, because Eq. (3) is also a soft limit and chiral limit result, giving the form factor $F_\gamma^{3\pi}(p_1, p_2, p_3)$ at the soft point.

In the QL model, the amplitude (3) is obtained by calculating the ''box'' graph, Fig. 1. This is not surprising, as the anomalous ''box'' amplitude (3) was already obtained analytically and exactly by Alkofer and Roberts [7] in the so-called Schwinger-Dyson (SD) ansatz approach, which is

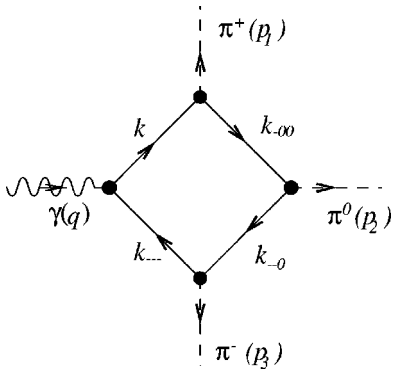

FIG. 1. One of the six box diagrams for the process $\gamma \to \pi^+\pi^0\pi^-$. The position of the u and d quark flavors on the internal lines, as well as Q_u or Q_d quark charges in the quark-photon vertex, varies from graph to graph, depending on the position of the quark-pion vertices.

more general. In this approach, one employs an ansatz for a dynamically dressed quark propagator, characterized by a momentum-dependent quark mass function $M(k^2)$ and by the related momentum-dependent quark-antiquark pseudoscalar pion bound state Bethe-Salpeter vertices Γ_{π^a} instead of our $g\gamma_5\tau_a$ quark-pion Yukawa couplings. The present free QL model, with its constant quark-pion coupling strength g and the free quark propagators $S(k)=i(\gamma\cdot k+M)/(k^2-M^2)$ containing constant effective constituent mass M, can therefore be considered as a special case of the SD ansatz approach, i.e., the simplest possible such ansatz.

Let us stress that for processes of the type $\gamma\to 3\pi$, going beyond the soft limit is much more important than for the process $\pi^0\to 2\gamma$ where the amplitude $T_\pi^{2\gamma}$ obtained in the chiral and soft limit is an excellent approximation for the realistic $\pi^0\to\gamma\gamma$ decay. By contrast, the current TJNAF measurement of the $\gamma\pi^+\to\pi^+\pi^0$ process [8], as well as already published [9] and still planned Primakoff measurements at CERN [10], involves so large values of energy and momentum transfer that departures from the soft-point result (3) may well be significant.

Nevertheless, to the best of our knowledge, no extension of Eq. (3) beyond the chiral and soft limit has been given in the QL (χQM, σ-model) approach so far, neither through a numerical calculation nor as an analytic result that would be the analogy of the amplitude (2) for the $\gamma\gamma$ decay of the massive pion. (In the SD approach [7], the box graph beyond the chiral and soft limit was addressed, but only numerically.) To fill this gap, which seems to exist in the literature even at the lowest nontrivial order, we provide such an analytic expression in the form of an expansion in powers of the pion momenta up to the eighth order, in addition to the numerical evaluation of the $\gamma\to 3\pi$ form factor accurate to all orders.

To compute the $\gamma\to 3\pi$ amplitude we use Eq. (1) in terms of the physical fields $\pi^\pm=(\pi_1\mp i\pi_2)/\sqrt{2}$ and $\pi^0\equiv\pi_3$, so that $\pi_a\tau_a=\sqrt{2}(\pi^+\tau_+ +\pi^-\tau_-)+\pi^0\tau_3$ where $\tau_\pm=(\tau_1\pm i\tau_2)/2$. There are six different contributing graphs, obtained from Fig. 1 by the permutations of the vertices of the three different pions. The momenta flowing through the four sections of the quark loop are conveniently given by various combinations of the symbols $\alpha,\beta,\gamma=+,0,-$ in $k_{\alpha\beta\gamma}\equiv k+\alpha p_1+\beta p_2+\gamma p_3$. Then, the anomalous vertex V_μ coupling $\pi^+\pi^0\pi^-$ to γ, viz., the scalar form factor $F_\gamma^{3\pi}(p_1,p_2,p_3)$ associated with it, is in the present approach calculated through the six VPPP box graphs as

$$\begin{aligned} V_\mu &= -i\epsilon_{\mu\nu\rho\sigma}p_1^\nu p_2^\rho p_3^\sigma F_\gamma^{3\pi}(p_1,p_2,p_3)\\ &= -i\epsilon_{\mu\nu\rho\sigma}p_1^\nu p_2^\rho p_3^\sigma f_\gamma^{3\pi}(p_1,p_2,p_3)\\ &\quad +(\text{permutations of } \pi^+,\pi^0,\pi^-), \end{aligned} \tag{4}$$

where the contribution of the first diagram (Fig. 1), $-i\epsilon_{\mu\nu\rho\sigma}p_1^\nu p_2^\rho p_3^\sigma f_\gamma^{3\pi}(p_1,p_2,p_3)$, is given by

$$\begin{aligned} &-\int\frac{d^4k}{(2\pi)^4}\mathrm{Tr}\{-ie\mathcal{Q}\gamma_\mu S(k_{---})\sqrt{2}g\gamma_5\tau_+ S(k_{--0})\\ &\quad\times g\gamma_5\tau_3 S(k_{-00})\sqrt{2}g\gamma_5\tau_- S(k)\}. \end{aligned} \tag{5}$$

The color and isospin traces are N_c and $\mathrm{Tr}_I(\mathcal{Q}\tau_+\tau_3\tau_-)=-2/3$, respectively. The Dirac trace is $-4iM\epsilon_{\mu\nu\rho\sigma}p_1^\nu p_2^\rho p_3^\sigma$, leading to the partial amplitude $f_\gamma^{3\pi}(p_1,p_2,p_3)=(+2/3)(eN_cg^3M/2\pi^2)I(p_1,p_2,p_3)$, where

$$\begin{aligned} &I(p_1,p_2,p_3)\\ &\quad\equiv -\frac{i}{\pi^2}\int\\ &\qquad\times\frac{d^4k}{(k^2-M^2)(k_{-00}^2-M^2)(k_{--0}^2-M^2)(k_{---}^2-M^2)}. \end{aligned} \tag{6}$$

After combining the four propagator denominators by the Feynman trick, and shifting k^μ by $p_1^\mu(1-x_3)+p_2^\mu(1-x_2)+p_3^\mu(1-x_1)$, the integral over the loop momentum k becomes

$$\begin{aligned} I(p_1,p_2,p_3) &= -\frac{i}{\pi^2}3!\int_0^1 dx_1\int_0^{x_1}dx_2\\ &\quad\times\int_0^{x_2}dx_3\int\frac{d^4k}{[k^2-R(p_1,p_2,p_3)^2]^4}\\ &= \int_0^1\int_0^{x_1}\int_0^{x_2}\frac{dx_3dx_2dx_1}{R(p_1,p_2,p_3)^4}\quad(\text{for } R^2>0), \end{aligned} \tag{7}$$

where

$$\begin{aligned} R(p_1,p_2,p_3)^2 &\equiv M^2-p_3^2x_1(1-x_1)-p_2^2x_2(1-x_2)\\ &\quad -p_1^2x_3(1-x_3)-2p_2\cdot p_3x_2(1-x_1)\\ &\quad -2p_1\cdot p_2x_3(1-x_2)-2p_1\cdot p_3x_3(1-x_1). \end{aligned} \tag{8}$$

Adding up the contributions from the remaining five diagrams yields the total amplitude

$$\begin{aligned} F_\gamma^{3\pi}(p_1,p_2,p_3) &= \left(\frac{eN_c}{2\pi^2}g^3M\right)\Bigg(+\frac{2}{3}\{I(p_1,p_2,p_3)\\ &\quad +I(p_1,p_3,p_2)+I(p_2,p_1,p_3)\}\\ &\quad -\frac{1}{3}\{I(p_3,p_1,p_2)+I(p_3,p_2,p_1)\\ &\quad +I(p_2,p_3,p_1)\}\Bigg). \end{aligned} \tag{9}$$

Since the integrals such as $I(p_1,p_2,p_3)$ are symmetric in the interchange of the first and third arguments, the two curly brackets in Eq. (9) are equal to each other. Therefore, the sum of the three u-quark ''box'' loop diagrams, as well as the sum of the three d-quark ones, gives contributions to the amplitude (9) which are separately symmetric under

$p_1\leftrightarrow p_2\leftrightarrow p_3$. For that reason, a calculation that would employ the integer charge isodoublet nucleons in the loops instead of the ones with quarks would—up to the fermion mass values M vs $M_{nucleon}$—give the same amplitude in spite of the three neutron graphs dropping out because of the vanishing neutron charge. Also, the interplay of the charge-isospin factors compensates the quark color factor $N_c=3$ as in the $\pi^0\to\gamma\gamma$ amplitude $T_\pi^{2\gamma}$, although the quark charges enter in $F_\gamma^{3\pi}$ linearly, and not quadratically.

The integrals appearing in Eq. (9), exemplified above by the one defined by Eqs. (6)–(8), are calculated in two ways. First, we calculate them numerically by the Gauss-Kronrod method. Second, we obtain the analytic expressions for $F_\gamma^{3\pi}$ [Eqs. (10),(12), (13), and (14) below] by expanding the integrands [exemplified by the one in the integral (6)–(8)] in the series of the scalar products of the pion momenta, $p_i\cdot p_j$ $(i,j=1,2,3)$. In this case, the analytic integration over x_1,x_2, and x_3 finally yields [to order $\mathcal{O}(p^4)$]

$$F_\gamma^{3\pi}(p_1,p_2,p_3)=\left(\frac{eN_c}{12\pi^2}\frac{g^3}{M^3}\right)\left(1+\frac{1}{3M^2}\{p_1\cdot p_2+p_1\cdot p_3+p_2\cdot p_3+p_1^2+p_2^2+p_3^2\}+\frac{1}{10M^4}\{p_1^4+p_2^4+p_3^4\}\right.$$
$$+\frac{1}{6M^4}\{p_1^2p_2^2+p_1^2p_3^2+p_2^2p_3^2\}+\frac{1}{5M^4}\{p_1\cdot p_2(p_1^2+p_2^2)+p_2\cdot p_3(p_2^2+p_3^2)+p_1\cdot p_3(p_1^2+p_3^2)\}$$
$$+\frac{1}{6M^4}\{p_2\cdot p_3p_1^2+p_1\cdot p_3p_2^2+p_1\cdot p_2p_3^2\}+\frac{1}{5M^4}\{p_1\cdot p_2p_1\cdot p_3+p_1\cdot p_2p_2\cdot p_3+p_1\cdot p_3p_2\cdot p_3\}$$
$$\left.+\frac{2}{15M^4}\{(p_1\cdot p_2)^2+(p_1\cdot p_3)^2+(p_2\cdot p_3)^2\}+\mathcal{O}(p^6)\right). \tag{10}$$

After using the GT relation, Eq. (10) returns at the soft point ($p_i=0$) the axial anomaly result (3). We introduce the form factor normalized to the anomaly amplitude (3), $\tilde{F}_\gamma^{3\pi}(p_1,p_2,p_3)=F_\gamma^{3\pi}(p_1,p_2,p_3)/F_\gamma^{3\pi}(0,0,0)$. It is also convenient to re-express the scalar products $p_i\cdot p_j$ through the Mandelstam variables as defined by Ref. [8]: $s=(p_1+p_2)^2$, $t'=(p_2+p_3)^2$, $u=(p_1+p_3)^2$, while $t=p_3^2$ serves as the measure of the virtuality of the third pion which may be off shell. The photon momentum is $q=p_1+p_2+p_3$.

We obtained the expansion for $F_\gamma^{3\pi}(p_1,p_2,p_3)$ to the order $\mathcal{O}(p^8)$ [relative to the anomaly result (3)], but give Eq. (10) only to the order $\mathcal{O}(p^4)$ for brevity as the $\mathcal{O}(p^8)$ expansion for general p_i is very lengthy. It will be given elsewhere. However, below we do give $F_\gamma^{3\pi}$ to the order $\mathcal{O}(p^8)$ for the simpler special cases which are important for comparing our predictions with the experiments [9,8,10]. Namely, one can take the photon to be on shell in all three pertinent experiments [9,8,10], in which at least two pion momenta, those of π^+ and π^0, are also on the mass shell. We thus set $q^2=0$ and $p_1^2=p_2^2=m_\pi^2$, whereby

$$s+t'+u\equiv p_1^2+p_2^2+p_3^2+q^2=2m_\pi^2+t. \tag{11}$$

In the Primakoff measurements [9,10], including the one [9] providing the only existing data point so far, the third pion is also on shell. Hence, $t=m_\pi^2$, in which case we predict

$$\tilde{F}_\gamma^{3\pi}(s,t')=\left(1+\frac{m_\pi^2}{2M^2}+\frac{m_\pi^4}{4M^4}+\frac{169m_\pi^6}{1260M^6}+\frac{193m_\pi^8}{2520M^8}\right)-\frac{m_\pi^2}{20M^4}\left(1+\frac{9m_\pi^2}{7M^2}+\frac{76m_\pi^4}{63M^4}\right)(s+t')+\frac{1}{60M^4}\left(1+\frac{9m_\pi^2}{7M^2}+\frac{94m_\pi^4}{63M^4}\right)$$
$$\times(s^2+t'^2)+\frac{1}{60M^4}\left(1+\frac{2m_\pi^2}{M^2}+\frac{341m_\pi^4}{126M^4}\right)st'-\frac{1}{252M^6}\left(1+\frac{29m_\pi^2}{10M^2}\right)(s^2t'+st'^2)-\frac{m_\pi^2}{315M^8}(s^3+t'^3)$$
$$+\frac{1}{1890M^8}(s^4+2s^3t'+3s^2t'^2+2st'^3+t'^4)+\mathcal{O}(p^{10}). \tag{12}$$

At CEBAF [8], one takes data near $t\approx -m_\pi^2$, for which our $\mathcal{O}(p^8)$ expansion yields

$$\tilde{F}_\gamma^{3\pi}(s,t') = \left(1+\frac{m_\pi^2}{6M^2}+\frac{m_\pi^4}{20M^4}+\frac{13m_\pi^6}{1260M^6}+\frac{m_\pi^8}{360M^8}\right) - \frac{m_\pi^2}{60M^4}\left(1+\frac{m_\pi^2}{3M^2}+\frac{8m_\pi^4}{63M^4}\right)s - \frac{m_\pi^2}{60M^4}\left(1+\frac{3m_\pi^2}{7M^2}+\frac{10m_\pi^4}{63M^4}\right)t'$$
$$+\frac{1}{60M^4}\left(1+\frac{3m_\pi^2}{7M^2}+\frac{13m_\pi^4}{63M^4}\right)s^2+\frac{1}{60M^4}\left(1+\frac{3m_\pi^2}{7M^2}+\frac{4m_\pi^4}{21M^4}\right)t'^2+\frac{1}{60M^4}\left(1+\frac{2m_\pi^2}{3M^2}+\frac{41m_\pi^4}{126M^4}\right)st'$$
$$-\frac{1}{252M^6}\left(1+\frac{29m_\pi^2}{30M^2}\right)(s^2t'+st'^2)-\frac{m_\pi^2}{945M^8}(s^3+t'^3)+\frac{1}{1890M^8}(s^4+2s^3t'+3s^2t'^2+2st'^3+t'^4)+\mathcal{O}(p^{10}), \tag{13}$$

where the $s\leftrightarrow t'$ symmetry is lost due to the virtuality $t=-p_1^2=-p_2^2=-m_\pi^2$ of the third pion.

Our momentum expansions (12) and (13) show clearly that the main contribution to the term linear in s and t' (dominating the s,t' dependence close to the soft limit) comes from $\mathcal{O}(p^4)$ and not $\mathcal{O}(p^2)$. This happens since the $\mathcal{O}(p^2)$ terms, due to the constraint (11), contribute only to the part independent of s and t'.

Note that in the on-shell case (12), the finite pion mass m_π causes a larger upward shift than in the off-shell case (13). For chiral pions ($m_\pi=0$) and real photons the condition (11) becomes $s+t'+u=t$. For this case, but for general t, the amplitude (9) becomes

$$\tilde{F}_\gamma^{3\pi}(s,t') = \left(1+\frac{t}{6M^2}+\frac{t^2}{30M^4}+\frac{t^3}{140M^6}+\frac{t^4}{630M^8}\right) - \frac{t}{60M^4}\left(1+\frac{3t}{7M^2}+\frac{t^2}{7M^4}\right)(s+t') + \frac{1}{60M^4}\left(1+\frac{3t}{7M^2}+\frac{11t^2}{63M^4}\right)$$
$$\times(s^2+t'^2)+\frac{1}{60M^4}\left(1+\frac{2t}{3M^2}+\frac{13t^2}{42M^4}\right)st' - \frac{1}{252M^6}\left(1+\frac{29t}{30M^2}\right)(s^2t'+st'^2) - \frac{t}{945M^8}(s^3+t'^3)+\frac{1}{1890M^8}$$
$$\times(s^4+2s^3t'+3s^2t'^2+2st'^3+t'^4)+\mathcal{O}(p^{10}), \tag{14}$$

showing that the $s\leftrightarrow t'$ symmetry is restored in the chiral limit. The massless pion amplitude (14) is smaller than the one with $m_\pi=138.5$ MeV by, typically, 4% when $M=m_\rho/2=385$ MeV, by some (depending on s) 6% when $M=330$ MeV, by more than 10% when $M=250$ MeV, etc. It is interesting that for small s and t', the chiral limit $F_\gamma^{3\pi}$ can fall slightly below its soft point value (3) when $t<0$.

In the CEBAF experiment [8], s will vary more than t'. For the t' range relevant at CEBAF, the t' dependence of $F_\gamma^{3\pi}$ anyway turns out to be rather weak. For example, suppose one plots (not done here to avoid overcrowding our figures) the $t=-m_\pi^2$ form factor (13) as a function of s for several values of t' varying from $t'=-m_\pi^2$ to $t'=-8m_\pi^2$. (Take $M=330$ MeV for definiteness.) One would thus get, across the whole s range relevant at CEBAF, a narrow strip of tightly spaced curves, where the curve depicting $\tilde{F}_\gamma^{3\pi}(s)$ for $t'=-8m_\pi^2$ would differ by just 2%–3% from the curve with $t'=-m_\pi^2$. In Figs. 2 and 3, we therefore show the dependence of $F_\gamma^{3\pi}$ (for various cases) on the variable s, with t' fixed. On the other hand, since t changes sign when we put also the third pion off shell as at CEBAF [8], the amplitude is more sensitive to this change.

In Fig. 2 we give our results at $t=-m_\pi^2$ (the t value most relevant at CEBAF [8]) for the constituent masses $M=385$ MeV, 330 MeV, 300 MeV, and 250 MeV. In fact, we show a pair of curves for each of these masses: one of the curves is obtained by exact numerical evaluation of the box amplitude, and the other corresponds to our series expansion to the order $\mathcal{O}(p^8)$. At the lowest depicted s, the form factor obtained by the accurate numerical calculation is (for each M) slightly below the corresponding series expansion approximating it, but exceeds it eventually as s grows. The convergence of the expansion is very satisfactory on the whole, since for $s\lesssim 11m_\pi^2$, the agreement between the two ways of calculation is very good for all these values of M. For $s>11m_\pi^2$, the exceptions are only the cases with unrealistically small M, such as $M=250$ MeV. For $M=250$ MeV, we plot the curves up to $s=s_{\rm tr}\approx 13.03m_\pi^2$ only. Namely, when s reaches $s_{\rm tr}=(2M)^2$, i.e., the threshold for production of an on-shell quark-antiquark pair, the QL approach becomes inadequate, because the amplitude starts being dominated by this threshold which is not physical but an artifact of the model (1). [Concerning the accuracy of the computations close to a threshold, the difficulty of numerical integration starts increasing gradually as one gets closer than m_π^2 to the threshold, while the accuracy of the $\mathcal{O}(p^8)$ expansion starts failing before that.]

Nevertheless, for the values of $s<16m_\pi^2$ accessible at CEBAF [8], such a threshold cannot be reached unless $M<2m_\pi=277$ MeV. Such values are, however, too low to serve as the constituent quark masses, which cannot be much lighter than $M\approx M_{nucleon}/3\approx 313$ MeV.

In Fig. 3 we compare our (numerically obtained) on-shell predictions for various M with the only existing experimental point so far [9] and with the predictions of chiral perturba-

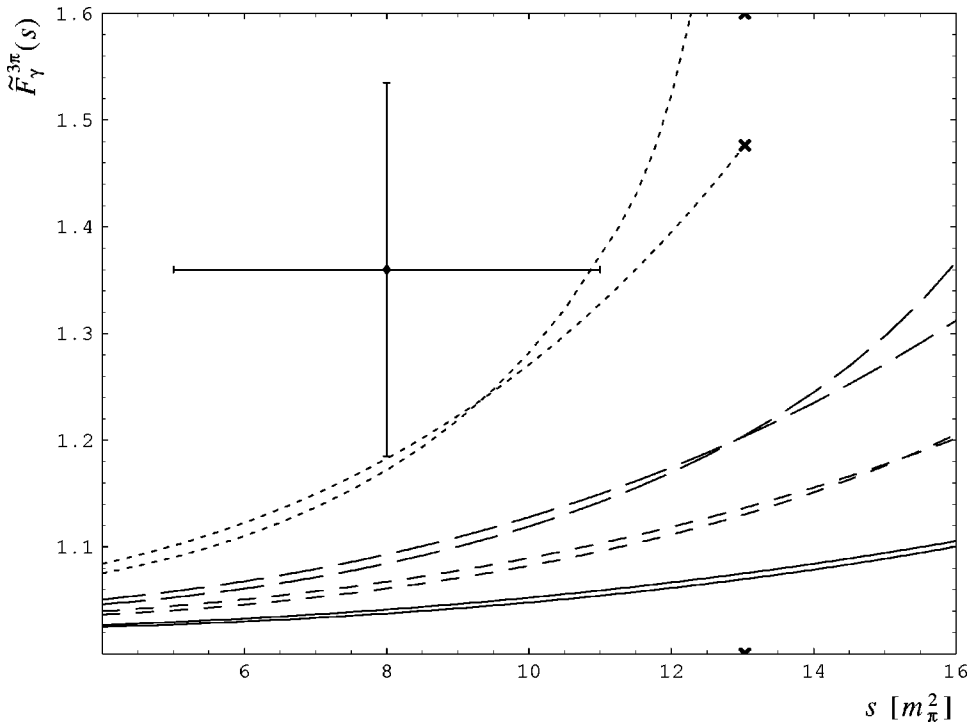

FIG. 2. Our numerically obtained $\gamma \to 3\pi$ form factors are compared with the corresponding $\mathcal{O}(p^8)$ expansions (13) for various values of M and $m_\pi = 138.5$ MeV. The corresponding pair of curves for $M = 385$ MeV is denoted by the solid lines, by the short-dashed lines for $M = 330$ MeV, by the long-dashed lines for $M = 300$ MeV, and by the very short-dashed lines (only up to $s_{\rm tr} = 13.03 m_\pi^2$, denoted by $\times$'s) for $M = 250$ MeV. The curves resulting from numerical integration start slightly below their respective power series at lowest values of the s variable, but then exceed the latter for sufficiently high s. All curves pertain to the off-shell case $t = -m_\pi^2$ (dominant at CEBAF [8], but not in the Serpukhov experiment [9] which provided the displayed data point, where $t = m_\pi^2$). The remaining variable t' is also set to $t' = -m_\pi^2$.

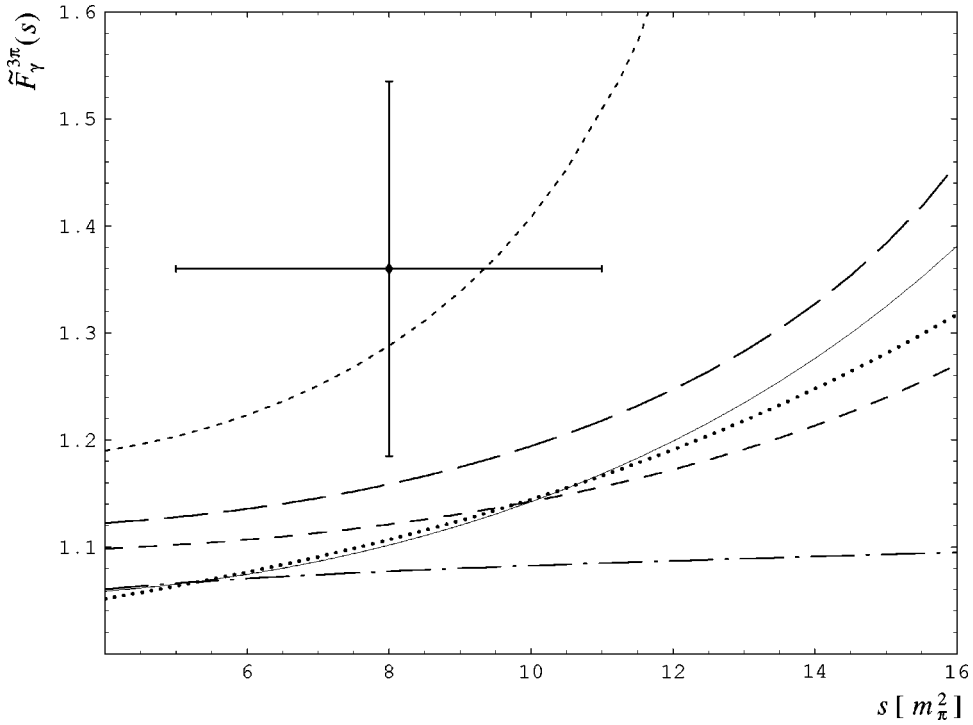

FIG. 3. The $\tilde{F}_\gamma^{3\pi}(s, t' = -m_\pi^2)$ predicted by VMD [13,12] (solid curve), VMD with final pion interactions [12] (dotted curve), and χPT [11,12] (dash-dotted curve) are compared with our $\tilde{F}_\gamma^{3\pi}(s, t' = -m_\pi^2)$ obtained by numerical integration for $M = 330$ MeV (short-dashed curve), $M = 300$ MeV (long-dashed curve), and $M = 250$ MeV (the topmost, very short-dashed curve). Same as the displayed data point [9], all curves pertain to all three pions on shell, so that $t = m_\pi^2 = (138.5\ \text{MeV})^2$. The remaining free variable t' is set to $t' = -m_\pi^2$ for all curves for definiteness.

tion theory (χPT) [11] [in Holstein's [12] renormalization convention—i.e., we take his [12] Eq. (10) for the χPT form factor], of vector meson dominance (VMD) [13] [Holstein's [12] Eq. (9)], and of VMD with the final pion rescattering included [12].

We conclude that our results agree rather well with VMD for constituent quark masses 300 MeV$<M<$330 MeV when $s>8m_\pi^2$. Going down in s, already at $s\sim 8m_\pi^2$ we agree rather well, but for somewhat higher M (330 MeV $\lesssim M\lesssim m_\rho/2$), with both VMD and χPT. For all s values shown, our predictions get somewhat closer to those of χPT when the ratio m_π^2/M^2 gets smaller, i.e., for the largest considered constituent quark mass, $M=m_\rho/2=385$ MeV. Since χPT results in the weakest momentum dependence, its predictions for the largest values of s accessible at CEBAF are significantly different from both VMD and our QL (χQM, σ-model) approach. The CEBAF experiment should thus be able to distinguish between these various physical mechanisms in this range of momenta. On the other hand, all these approaches agree reasonably well for the lowest of s values accessible at CEBAF. In particular, our approach agrees with VMD and χPT, that the existing data point [9] is probably an overestimate, as we can fit it well (e.g., with the $M=250$ MeV curve in Fig. 3) only for unrealistically low values of M.

The authors thank R. Alkofer and D. Kekez for many helpful discussions, and K. Kumerički for checking the manuscript. The support of the Croatian Ministry of Science and Technology contract 1-19-222 is also acknowledged.

[1] S. L. Adler, Phys. Rev. **177**, 2426 (1969).
[2] J. S. Bell and R. Jackiw, Nuovo Cimento A **60**, 47 (1969).
[3] J. Steinberger, Phys. Rev. **76**, 1180 (1949).
[4] A. A. Andrianov, D. Espriu, and R. Tarrach, Nucl. Phys. **B533**, 429 (1998).
[5] Ll. Ametller, L. Bergström, A. Bramon, and E. Massó, Nucl. Phys. **B228**, 301 (1983).
[6] S. L. Adler, B. W. Lee, S. Treiman, and A. Zee, Phys. Rev. D **4**, 3497 (1971); M. V. Terent'ev, Phys. Lett. **38B**, 419 (1972); R. Aviv and A. Zee, Phys. Rev. D **5**, 2372 (1972).
[7] R. Alkofer and C. D. Roberts, Phys. Lett. B **369**, 101 (1996).
[8] R. A. Miskimen, K. Wang, and A. Yagneswaran (spokesmen), ''Study of the Axial Anomaly using the $\gamma\pi^+\to\pi^+\pi^0$ Reaction Near Threshold,'' letter of intent, CEBAF-experiment 94-015.
[9] Yu. M. Antipov Phys. Rev. D **36**, 21 (1987).
[10] M. A. Moinester, V. Steiner, and S. Prakhov, in Hadron-Photon Interactions in COMPASS, proceedings of 37th International Winter Meeting on Nuclear Physics, Bormio, Italy, 1999, edited by I. Iori, Ricerca Scientifica ed Educazione Permanente Supplemento, No. 114, hep-ex/9903017.
[11] J. Bijnens, A. Bramon, and F. Cornet, Phys. Lett. B **237**, 488 (1996).
[12] B. Holstein, Phys. Rev. D **53**, 4099 (1996).
[13] S. Rudaz, Phys. Lett. **145B**, 281 (1984); T.D. Cohen, Phys. Lett. B **233**, 467 (1989).